Scar imaging in the dyssynchronous left ventricle: Accuracy of myocardial metabolism by positron emission tomography and function by echocardiographic strain

Camilla Kjellstad Larsen [a,b], Elena Galli [c], Jürgen Duchenne [d], John M. Aalen [a,b], Caroline Stokke [e,f], Jan Gunnar Fjeld [e,g], Ganna Degtiarova [h], Piet Claus [h], Olivier Gheysens [i], Jorg Saberniak [j], Per Anton Sirnes [k], Erik Lyseggen [b], Jan Bogaert [l], Erik Kongsgaard [b], Martin Penicka [m], Jens-Uwe Voigt [d], Erwan Donal [c], Einar Hopp [e], Otto A. Smiseth [a,b,*]

[a] Institute for Surgical Research, Oslo University Hospital and University of Oslo, Oslo, Norway
[b] Department of Cardiology, Oslo University Hospital, Oslo, Norway
[c] Department of Cardiology, University Hospital of Rennes and University of Rennes, Rennes, France
[d] Department of Cardiovascular Diseases, University Hospitals Leuven and Department of Cardiovascular Sciences, KU Leuven – University of Leuven, Leuven, Belgium
[e] Division of Radiology and Nuclear Medicine, Oslo University Hospital, Oslo, Norway
[f] Department of Physics, University of Oslo, Oslo, Norway
[g] Oslo Metropolitan University, Oslo, Norway
[h] Department of Nuclear Medicine, University Hospitals Leuven and Department of Imaging and Pathology, KU Leuven – University of Leuven, Leuven, Belgium
[i] Department of Nuclear Medicine, Cliniques Universitaires Saint-Luc and Institute of Clinical and Experimental Research (IREC), Université Catholique de Louvain, Brussels, Belgium
[j] Department of Cardiology, Akershus University Hospital, Lorenskog, Norway
[k] Ostlandske Hjertesenter, Moss, Norway
[l] Department of Radiology, University Hospitals Leuven, Leuven, Belgium
[m] Cardiovascular Center, OLV Clinic, Aalst, Belgium

A R T I C L E   I N F O

A B S T R A C T

Purpose: Response to cardiac resynchronization therapy (CRT) is reduced in patients with high left ventricular (LV) scar burden, in particular when scar is located in the LV lateral wall or septum. Late gadolinium enhancement (LGE) cardiac magnetic resonance (CMR) can identity scar, but is not feasible in all patients. This study investigates if myocardial metabolism by ^{18}F-fluorodeoxyglucose positron emission tomography (FDG-PET) and contractile function by echocardiographic strain are alternatives to LGE-CMR.
Methods: In a prospective multicenter study, 132 CRT candidates (91% with left bundle branch block) were studied by speckle tracking strain echocardiography, and 53 of these by FDG-PET. Regional myocardial FDG metabolism and peak systolic strain were compared to LGE-CMR as reference method.
Results: Reduced FDG metabolism (<70% relative) precisely identified transmural scars (≥50% of myocardial volume) in the LV lateral wall, with area under the curve (AUC) 0.96 (95% confidence interval (CI) 0.90–1.00). Reduced contractile function by strain identified transmural scars in the LV lateral wall with only moderate accuracy (AUC = 0.77, CI 0.71–0.84). However, absolute peak systolic strain >10% could rule out transmural scar with high sensitivity (80%) and high negative predictive value (96%). Neither FDG-PET nor strain identified septal scars (for both, AUC < 0.80).
Conclusions: In CRT candidates, FDG-PET is an excellent alternative to LGE-CMR to identify scar in the LV lateral wall. Furthermore, preserved strain in the LV lateral wall has good accuracy to rule out transmural scar. None of the modalities can identify septal scar.

---

1. Introduction

Cardiac resynchronization therapy (CRT) is an established treatment for patients with symptomatic heart failure, reduced left ventricular (LV) ejection fraction (EF) and broad QRS, preferably with left bundle branch block (LBBB) morphology. Nevertheless, CRT fails to improve symptoms in one-third of the patients, and reduced therapeutic response is related to LV scar burden [1,2]. As shown by Bleeker et al., who evaluated myocardial scar by late gadolinium enhancement cardiac magnetic resonance (LGE-CMR), patients with transmural scar in the LV posterolateral wall have markedly reduced clinical response and attenuated LV reverse remodeling after CRT [3]. Furthermore, as shown recently by our group in a prospective, multicenter study, septal scar is associated with poor response to CRT [4]. Therefore, identification of scar in the LV lateral wall and septum may aid in selecting patients who are likely to respond to CRT.

Cardiac magnetic resonance (CMR) with late gadolinium enhancement (LGE) is the clinical gold standard for myocardial scar [5], but is not feasible in all patients, and is limited by accessibility. Therefore, there is need for alternative methods to image myocardial scar. In the present study, we investigate if myocardial glucose metabolism by positron emission tomography (PET) with ^{18}F-fluorodeoxyglucose (FDG) can identify LV myocardial scars in patients with LBBB or other causes of LV intraventricular conduction delay, who are referred for CRT. Additionally, we investigate if myocardial contractile function measured by echocardiographic strain imaging can be used to identify scar.

The principle behind FDG-PET to identify scar, is that myocardial uptake of the radioactive glucose analogue reflects metabolic activity, i. e. viability of the myocardium. Myocardial shortening by strain imaging is directly related to viability since non-viable myocardium does not contract and when only part of the wall is viable, there is reduced contraction as reflected in reduced systolic strain. In CRT candidates, however, scar imaging by FDG-PET and strain may be challenging, as LBBB markedly alters myocardial function and metabolism [6–8]. No previous study has validated scar imaging by FDG-PET against LGE-CMR in CRT candidates. Scar imaging by strain imaging has been compared to LGE-CMR in ischemic cardiomyopathy [9–11], but not in non-ischemic cardiomyopathy, which represent a large fraction of patients who receive CRT.

The objectives of the present study were to determine if assessment of myocardial metabolism by FDG-PET and LV systolic function by strain echocardiography can identify LV scar in patients referred for CRT. As reference method for scar, we used LGE-CMR.

2. Methods

2.1. Study population

From a prospective, multicenter CRT study, we consecutively included all patients with QRS width > 120 ms and available LGE-CMR scan ($n = 132$). The background for not performing LGE-CMR has been described previously [4]. Criteria for LBBB was according to guidelines of the European Society of Cardiology [1]. Reversible ischemia was excluded by clinical history taking, supplemented with coronary angiography if considered necessary by the treating physician. Inclusion criterion was indication for CRT according to 2013 European Society of Cardiology guidelines. LGE-CMR served as reference standard for scar. All 132 patients underwent echocardiography and 53 of these were studied by FDG-PET.

The study was conducted following the "Good Clinical Practice" guidelines of the Declaration of Helsinki and was approved by the Regional Ethical Committees of every participating center. All patients gave their written informed consent for study participation. The present study is part of the clinical study "Contractile Reserve in Dyssynchrony: A Novel Principle to Identify Candidates for Cardiac Resynchronization Therapy (CRID–CRT)", which was registered at clinicaltrials.gov (identifier NCT02525185).

2.2. Cardiac magnetic resonance (CMR)

The CMR imaging was performed as previously described [4]. An experienced radiologist in a designated core lab, blinded to other results, determined if LGE was present and if so, whether distribution was consistent with ischemic etiology or not. All LGE, independent of etiology, was quantified with a specific analysis tool [12]. Transmural segmental scar was pre-specified as LGE $\geq$ 50% of segmental volume, and non-transmural segmental scar as <50% of segmental volume, irrespective of wall thickness. Heart failure etiology was considered ischemic if history of previous myocardial infarction and/or significant coronary artery disease by angiography, and if LGE pattern with scar extending from the subendocardium, consistent with previous infarction.

2.3. Nuclear imaging

Glucose metabolism was assessed by FDG-PET. Scanners were Biograph 64 or 16 HiRez PET/computer tomography (CT) (Siemens, Erlangen, Germany) and Discovery MI PET/CT (GE Healthcare, Chicago, Illinois, US). The investigation was performed during resting conditions and the patients were instructed to avoid exercise the days before. Patient preparation consisted of a hyperinsulinemic euglycemic clamping method [13] or an oral glucose loading protocol. After stabilization of the glucose levels, 370 MBq FDG was administered and a 40-min acquisition was performed 45 min after injection.

PET-images were reconstructed using ordered-subsets expectation maximization algorithms (4 iterations and 8 subsets), matrix size 256 $\times$ 256, and a 5.0 mm Gaussian filter. Attenuation correction was performed. A trained reader in a designated core lab, blinded to other results, performed the PET analyses. Segmental values were reported as percentage of the segment with highest mean tracer uptake.

2.4. Echocardiographic analysis

A Vivid E9 or E95 ultrasound scanner (GE Vingmed Ultrasound, Horten, Norway) was used for two-dimensional (2D) grey-scale echocardiographic acquisitions from the apical views. Average frame rate was 65 ± 10 /s. Ventricular volumes and LV ejection fraction were calculated by the biplane Simpson's method. Blood pressure was measured non-invasively at examination start.

Longitudinal strain was measured by speckle tracking echocardiography (Echopac, GE Vingmed Ultrasound, Horten, Norway). Peak systolic strain was defined as maximum negative value prior to aortic valve closure (AVC). Post-systolic shortening was measured as shortening after AVC. Radial strain measurements were attempted, but was often unsuccessful due to thin LV wall in many patients. Therefore, radial strain is not part of this study. A trained reader in a designated core lab, blinded to other results, performed the strain analyses.

An index of segmental myocardial work was calculated by LV pressure-strain analysis using a semi-automated analysis tool (Echopac,

version 202, GE Vingmed Ultrasound, Horten, Norway) and a non-invasive estimate of LV pressure (14).

All investigated parameters (CMR, nuclear and echocardiographic) were reported on a segmental level using the 17 segment model (15), where all segments except the apex (segment 17) were analyzed. Analyses were performed on a segmental level. In total, 2112 segments (132 patients × 16 segments per patient) were available for analysis. In one patient, we excluded six segments from LGE analysis because of regional artefacts from pacemaker leads. Of the remaining 2106 segments, 108 were excluded from strain and work analysis due to inadequate echocardiographic image quality. All 848 segments (53 patients × 16 segments per patient) available for PET analyses were studied. The ratio between septal metabolism and myocardial work was calculated for each segment.

Echocardiography was performed within a time range of 24 h and PET within 5 days from the CMR examination.

2.5. Statistical analyses

Continuous variables are expressed as mean ± standard deviation (SD) if normally distributed, otherwise as median (10, 90% percentile). Comparisons between groups were made by Student's t-test or Mann-Whitney U test, as appropriate. Statistical significance was set at a two-tailed probability level of $p < 0.05$. Each parameter's ability to detect scar was evaluated by receiver operating characteristic (ROC) curves with calculation of area under the curve (AUC). SPSS version 25.0 (IBM Corporation, Armonk, NY) was used for analyses.

3. Results

3.1. Study population

Patient characteristics, number of interpretable segments and number of scarred segments in each LV region are presented in Table 1. Mean QRS-width was 164 ± 17 ms, and 91% had LBBB, with 95% in sinus rhythm and 5% in atrial fibrillation. Mean LV EF was 30 ± 8% and average NYHA functional class 2.3 ± 0.6.

Myocardial scar by FDG-PET.

Table 1
Patient characteristics.

Variable	Average ± SD
Age (years)	66 ± 10
Male sex (%)	67
Heart failure etiology (no)	
Ischemic	55 (42%)
Non-ischemic	77 (58%)
Rhythm	
Sinus rhythm (%)	95
Atrial fibrillation (%)	5
QRS duration (milliseconds)	164 ± 17
QRS configuration (%)	
LBBB	91
Non-LBBB	9
Systolic blood pressure (mmHg)	126 ± 21
Diastolic blood pressure (mmHg)	70 ± 12
LV End diastolic volume (milliliter)	201 ± 76
LV Ejection fraction (%)	30 ± 8
Segments available for scar analysis (no)	Segments with non-transmural/transmural scar (no)
Lateral wall (660)	96/44
Septum (657)	170/40
Anterior wall (393)	88/24
Inferior wall (396)	106/34

LBBB = left bundle branch block; LV = left ventricular.

Fig. 1 shows FDG-PET images from 3 representative patients: one with no scar, one with scar in the lateral wall and one with septal scar. In the patient with no scar, the figure shows markedly asymmetric distribution of myocardial glucose metabolism, with hypo-metabolism in the septum relative to the LV lateral wall. The figure also illustrates that lateral wall scar was associated with marked reduction in glucose metabolism in the lateral wall. Numbers are given in Table 2.

FDG-PET identified transmural scars (LGE ≥ 50%) in the LV lateral wall with high accuracy (AUC = 0.96, 95% CI 0.90–1.00) (Table 3 and 4, Figs. 1 and 2). By ROC curve analysis, optimal cut off to identify transmural scar in the LV lateral wall was glucose uptake <70% relative to the segment with highest uptake. Using this cut off, sensitivity and specificity for identifying transmural scar was 94% and 91%, respectively. Replacing the statistically optimal threshold value with a cut off value of 50% FDG uptake, yielded a very high specificity (99%), but at the expense of a much lower sensitivity (56%).

In septal segments with no scar, glucose metabolism was reduced to 52% (95% CI: 25–86%) relative to the segment with highest uptake, generally located in the LV lateral wall. In septal segments with transmural scar, metabolism was further reduced to 42% (95% CI: 21–74%), $p = 0.012$. As indicated by the confidence intervals, there was substantial overlap between metabolism in normal septal segments and those with myocardial scar (Table 2). Therefore, FDG-PET could not identify septal scar. This is illustrated in Fig. 2, which shows weak association between glucose metabolism by FDG-PET and scar by LGE-CMR.

With regard to non-transmural scars, neither septal nor LV lateral wall scars were identified by FDG-PET (Table 3).

3.2. Myocardial scar by strain imaging

Peak systolic strain differed markedly between the LV lateral wall and septum (Table 2). In ventricles with no scar, peak lateral wall strain was −12.6% (95% CI: −1.3 to −24.7), whereas peak septal strain was −8.9% (95% CI: −0.4 to −20.1) ($p < 0.001$). As expected, in both LV lateral wall and septal segments, transmural scars were associated with reductions in absolute values of peak systolic strain (Table 2).

Fig. 3 shows individual values of peak systolic strain in LV lateral wall segments with different degrees of scar. The accuracy to identify lateral wall transmural scar by peak systolic strain was moderate, with AUC of 0.77 (95% CI: 0.71–0.84). However, absolute peak systolic strain >10% identified lateral wall segments without transmural scar with high sensitivity (80%) and high negative predictive value (96%). Values of absolute strain <10%, however, were inconclusive with regard to transmural scar (Fig. 3, Table 4). We also tested if post-systolic strain could identify myocardial scar, but this parameter provided no added value compared to measuring peak systolic strain (Table 2).

For the septum, however, there were relatively weak associations between peak systolic strain and transmural scar, with AUC 0.69 (95% CI: 0.60–0.78), indicating low accuracy of peak systolic strain to identify transmural septal scars. With regard to non-transmural scars, they were not identified by strain imaging in the septum or LV lateral wall.

We also investigated if myocardial work index, as an additional parameter of myocardial function, could identify segments with myocardial scar. LV lateral wall segments with transmural scar had lower ($p < 0.001$) values for positive work (1020 mmHg·% (95% CI: 85–2348) than lateral segments with no scar (1729 mmHg·% (95% CI: 425–3577). Similarly, in the septum, absence of scar was associated with increased (p < 0.001) positive myocardial work of 881 mmHg·% (95% CI: 178–2176), as compared to 583 mmHg·% (95% CI: 127–1532) in septal segments with transmural scar. When comparing ability to identify scar, however, septal and lateral wall work indices were not superior to peak systolic strain and therefore provided no added value.

The asymmetry in FDG metabolism correlated with asymmetry in workload ($r = 0.44$, $p = 0.001$, Fig. 4).
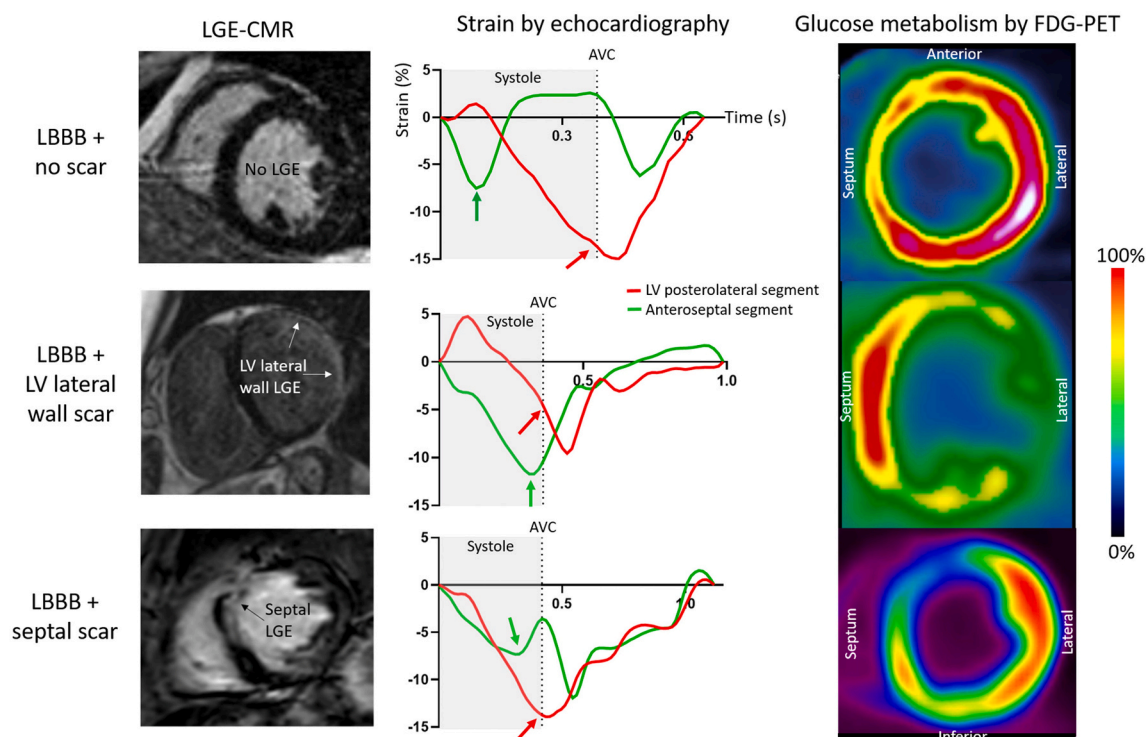
Fig. 1. Recordings from representative patients: The images are from patients where LGE-CMR shows no myocardial scar (upper panels), transmural scar in the LV lateral wall (middle panels) and transmural scar in the septum (lower panels). Green and red arrows indicate peak systolic strain for septum and the LV lateral wall, respectively. The anteroseptal and posterolateral segments are used.

The three patients illustrate typical spatial non-uniformities in distributions of LV myocardial metabolism and strain in patients with different locations of LV scar. The patient with no scar has markedly reduced septal strain and metabolism relative to the LV lateral wall. In the patient with lateral wall scar there is reduction in both metabolism and strain in the lateral wall relative to septum. In the patient with septal scar, there are reductions in both septal metabolism and strain. Please note that the patient with no septal scar has approximately similar reduction in peak systolic strain as the patient with septal scar, and both patients have reductions in septal metabolism relative to the lateral wall.

LV = left ventricular, LBBB = left bundle branch block, LGE-CMR = late gadolinium enhancement cardiac magnetic resonance, FDG-PET = ^{18}F-fluorodeoxyglucose Positron Emission Tomography, AVC = aortic valve closure. (For interpretation of the references to colour in this figure legend, the reader is referred to the web version of this article.)

Table 2
Strain and glucose metabolism in segments with varying degree of scar.

Variable	Lateral wall			Septum		
	No scar	Non-transmural scar	Transmural scar	No scar	Non-transmural scar	Transmural scar
Peak negative systolic strain (%)	−12.6 (−1.3 to −24.7)	−9.0* (0.0 to −22.8)	−6.2*† (−0.0 to −15.8)	−8.9 (−0.4 to −20.1)	−8.4 (−0.7 to −19.7)	−5.6*† (−0.1 to −14.6)
Post systolic strain (%)	−2.0 (0.0 to −8.1)	−2.5* (0.0 to −8.0)	−4.0*† (0.0 to −14.0)	−4.0 (0.0 to −11.5)	−2.9* (0.0 to −8.6)	−3.1 (0.0 to −13.3)
Glucose metabolism (%)	86.5 (63.9 to 100.0)	81.7* (46.2 to 100.0)	48.4*† (26.0 to 85.8)	51.5 (25.0 to 85.7)	54.2 (19.3 to 98.3)	41.8*† (21.1 to 73.7)

Values are given in average (95% confidence interval). * = $p < 0.05$ compared to segments without scar. † = $p < 0.05$ compared to segments with non-transmural scar.

Table 3
The ability of strain and metabolism to identify scarred segments by receiver operating characteristic curve analysis.

	Area under the curve (95% confidence interval)	
	Non-transmural scar	Transmural scar
Lateral wall		
Peak negative systolic strain	0.67 (0.61–0.73) [94]	0.77 (0.71–0.84) [44]
Glucose metabolism	0.58 (0.49–0.67) [54]	0.96 (0.90–1.00) [16]
Septum		
Peak negative systolic strain	0.53 (0.48–0.58 [165]	0.69 (0.60–0.78) [39]
Glucose metabolism	0.53 (0.48–0.61) [77]	0.68 (0.57–0.79) [21]

Only the parameters that best identified scars in each region are included in the table. Number of scarred segments for each analysis in square brackets.

4. Discussion

From this prospective multicenter study, we present the novel finding that FDG-PET identifies LV lateral wall scar with high accuracy in patients with LBBB. These results imply that FDG-PET represents an alternative to LGE-CMR for scar imaging in CRT candidates. The other novel finding is that preserved peak systolic strain (>10%) in the LV lateral wall excludes transmural scar with high accuracy. A more marked reduction in systolic strain was nonspecific regarding scar detection.

In our study population, there were marked reductions in septal metabolism and function caused by the abnormal electrical activation. Patients with septal scarring had additional reductions in function and
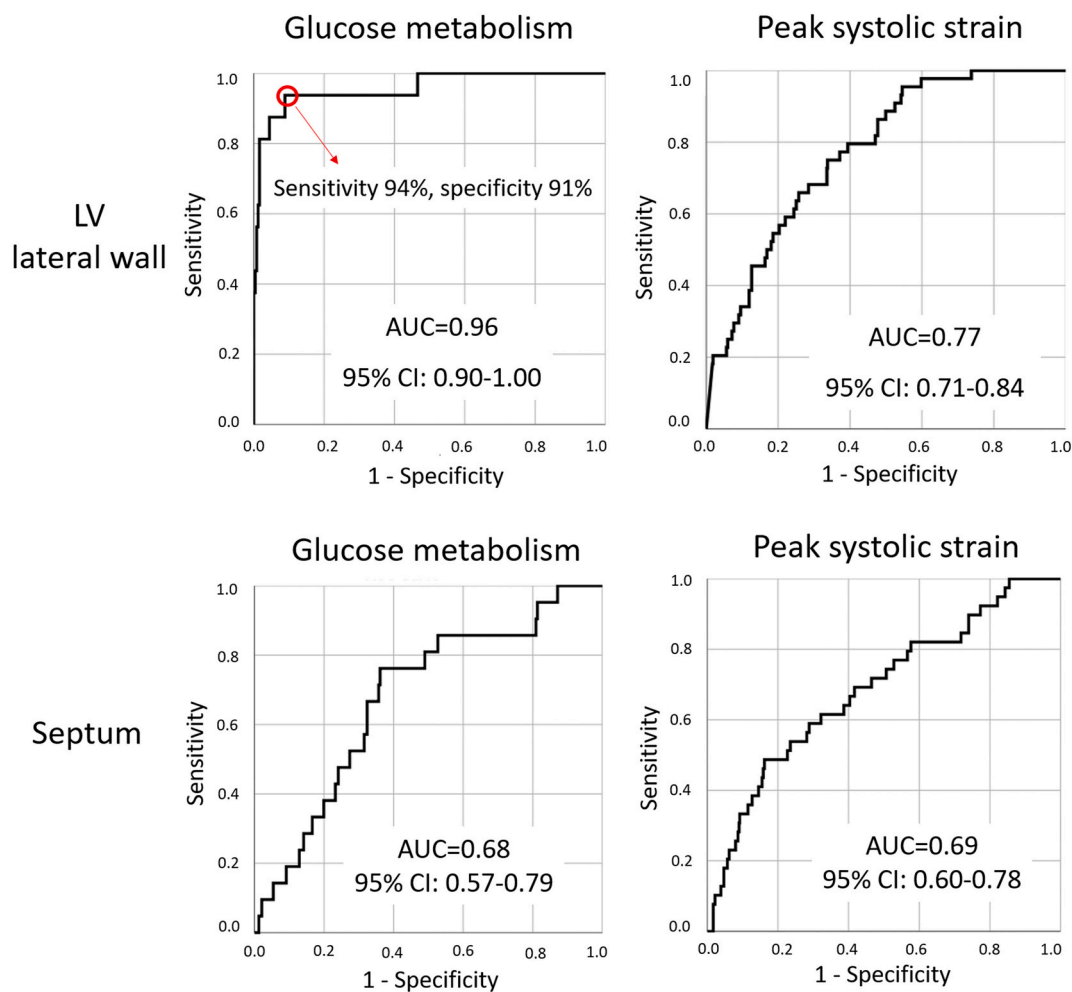
Table 4

The ability of peak systolic strain and glucose metabolism to identify segmental transmural scars (LGE ≥ 50%) in the lateral wall and septum, and their derived optimal cut offs.

	Cut off	Sensitivity (%)	Specificity (%)	PPV (%)	NPV (%)	Accuracy (%)
Peak negative systolic strain	%					
- Lateral wall	−10.2	80	61	18	96	78
- Septum	−7.1	69	58	11	96	69
Glucose uptake	%					
- Lateral wall	69.6	94	91	41	100	91
- Septum	44.1	76	64	16	97	65

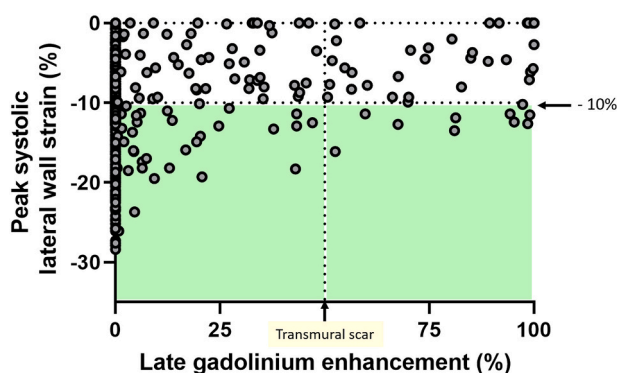LGE = late gadolinium enhancement; PPV = positive predictive value; NPV = negative predictive value.

Fig. 2. ROC curves of the ability of peak systolic strain and glucose metabolism to identify transmural scars (LGE ≥50%) in the LV lateral wall and septum. Glucose metabolism by FDG-PET predicted transmural scars in the LV lateral wall with high accuracy, with glucose uptake of 70% as optimal cut off. Myocardial strain and work by echocardiography were less precise. Neither FDG-PET (glucose metabolism) nor echocardiographic parameters identified transmural septal scars. ROC = receiving operating characteristic; LGE = late gadolinium enhancement; LV = left ventricular; FDG-PET = ^{18}F-fluorodeoxyglucose Positron Emission Tomography; AUC = area under the curve; CI = confidence interval.

metabolism, and neither FDG-PET nor strain imaging could differentiate between changes in metabolism and function due to scarring and electrical dyssynchrony. This was evident as marked overlap between values for glucose metabolism and strain in patients with and without transmural septal scars. Therefore, none of the imaging modalities FDG-PET and systolic strain could identify scar tissue in the septum.

4.1. Nuclear imaging

In the present study, optimal cut-off for FDG uptake to identify transmural scar in the LV lateral wall was 70% calculated relative to the segment with highest uptake. Previous studies in patients with coronary disease have found somewhat lower cut-offs ([16]). This apparent inconsistency may be related to the abnormal distribution of myocardial metabolism in LBBB, with relative hypo-metabolism in the septum compared to the LV lateral wall. Our results shows that a lower cut off (50% FDG uptake) identifies transmural lateral wall scar with lower sensitivity. Hence, clinically relevant scars is likely to go unrecognized using this lower cut off in the present patient population. Of note, our results only suggest using the threshold of 70% FDG uptake to identify

Fig. 3. Relationship between peak systolic strain and percentage LGE (scar) in lateral wall segments.

Peak absolute strain <10% was nonspecific with regard to scar extension by late gadolinium enhancement. As indicated by the green-enhanced area, absolute peak systolic strain >10% correctly classified segments with regard to transmurality in a majority ($n = 356$) of segments and incorrectly in only a few ($n = 10$). (For interpretation of the references to colour in this figure legend, the reader is referred to the web version of this article.)
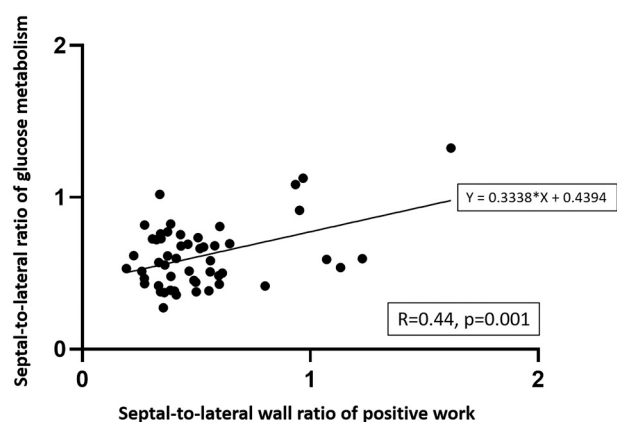
Fig. 4. Correlation between asymmetry in work and metabolism between septum and the lateral wall.

The asymmetry in metabolism between septum and LV lateral wall correlated significantly with the asymmetry in workload. One outlier was excluded.

transmural lateral wall scars, not to identify less extensive scarring or scarring in other myocardial region.

We have previously shown that high glucose metabolism in the LV lateral wall (relative to septum) predicts CRT response [17].

Inability to detect septal scars by FDG-PET is most likely related to altered mechanical function in the septum, which impacts metabolism. As proposed by Prinzen et.al [6], reduced septal work in the dyssynchronous ventricle reduces metabolic demand, which explains the reduced glucose metabolism in septum relative to the lateral wall [7]. These experimental data are supported by our observations of a significant association between asymmetry in work and asymmetry in metabolism between septum and the LV lateral wall. As suggested by our study in dyssynchronous ventricles, FDG-PET cannot differentiate between reductions in glucose metabolism caused by septal scar and reduced metabolic demand due to reduction in septal work load.

4.2. Echocardiographic strain imaging

The demonstration that *preserved* strain in the LV lateral wall could rule out transmural scar is consistent with observations in previous studies of radial strain that were limited to ischemic cardiomyopathy [11]. In the present study, however, *reduced* lateral wall strain (≤10%)

was nonspecific with regard to the presence of lateral wall scar. This is in apparent conflict with previous studies limited to ischemic cardiomyopathy, which have shown a strong association between radial [10,18] and longitudinal [9] strain in the LV lateral wall and transmural scar. However, not all studies used LGE-CMR as reference standard for scar and suggested cut offs for strain varies between studies. In patients with non-ischemic cardiomyopathy, there is typically reduction in LV shortening in all or most segments regardless of tissue viability. This probably explains why low values of lateral wall strain had no diagnostic value as marker of myocardial scar in our patient group. Taken together, the observations in the present study show that preserved myocardial strain in the LV lateral wall can be used to rule out transmural scar, which may be useful when considering LV electrode placement in the LV lateral wall in CRT candidates.

4.3. Alternative methods to image scar in dyssynchronous ventricles

Studies in patients with coronary disease show that PET perfusion imaging, and single photon emission computed tomography (SPECT) are comparable to FDG-PET in viability diagnostics [16]. However, it remains to be tested how accurate these imaging modalities are for assessment of LV scar in patients with heart failure and LBBB. A previous study in patients with LBBB indicates that resting SPECT images may show fixed perfusion defects that may be misinterpreted as septal scar [19]. Importantly, several studies confirm the utility of applying myocardial perfusion imaging by SPECT to predict response to CRT [20–22]. Furthermore, SPECT is less expensive and more available than PET, which, like CMR, is limited by accessibility.

In the present study, we used longitudinal strain to evaluate LV function. In principle, LV radial strain should give similar results since deformation in the long axis is always accompanied by deformation in the short axis (conservation of mass). In the present study, however, we found longitudinal strain easier to perform, probably due to markedly dilated ventricles with wall thinning.

Traditional echocardiographic parameters such as LV wall thickness and wall motion score may also be used to evaluate myocardial scar, but these methods are challenging to use in the dyssynchronous heart.

4.4. Clinical implications

Selecting patients for CRT based on scar characterization in the LV lateral wall and septum may improve responder rates to the therapy. Our findings that FDG-PET is a good alternative to LGE-CMR to identify transmural LV lateral wall scar in these patients, is clinically relevant, for example in patients where LGE-CMR is contraindicated. Furthermore, well-preserved LV lateral wall strain indicates that transmural scar in this region is unlikely. Reduced LV lateral wall strain, on the other hand, is not conclusive of scar and should be interpreted with caution. Recent studies have demonstrated that septal scar by CMR combined with information on either LV workload by echocardiography [4] or glucose metabolism by FDG-PET [17], accurately identifies CRT responders. Both approaches rely on LGE-CMR to identify septal scar, in line with findings from the present study that neither echocardiography nor PET can reliably assess scars in septum.

4.5. Limitations

The PET imaging part of the study was of moderate size, and a larger study population may have provided additional information, in particular for assessment of non-transmural scars. Increased FDG uptake due to reversible ischemia may affect the number of LV lateral wall segments with FDG uptake <70%. However, included patients had no history of reversible ischemia, were instructed to avoid exercise the days before, and the investigations were performed under resting conditions. Furthermore, patient preparation was performed to ensure globally high glucose uptake within the myocardium, minimizing the potential effect

of this confounder. In total, with regard to transmural scars in the LV lateral wall, the data were convincing and clearly showed the utility of FDG-PET as an alternative to LGE-CMR. It does not seem likely that a larger study would have given different results for FDG-PET imaging of septal scars since differentiation between reduced metabolism due to reduced septal work caused by dyssynchrony, would not be easy to separate from reduced metabolism due to reduced mass of viable myocardium.

The present study did not include nuclear perfusion imaging which could potentially provide additional information regarding septal scar. In principle, however, a similar limitation as for FDG-PET may apply to perfusion imaging since myocardial microvascular flow is autoregulated and determined by metabolism.

5. Conclusions

We present the novel finding that FDG-PET is an excellent modality to identify scar in the LV lateral wall in CRT candidates, and is therefore an alternative to LGE-CMR. Myocardial strain imaging by speckle tracking echocardiography also provides important diagnostic information as preserved strain in the LV lateral wall has good accuracy to rule out transmural scar. None of the modalities could identify septal scar because reductions in metabolism and strain due to abnormal electrical activation, overlapped with reductions due to scar. Therefore, currently LGE-CMR is the only clinical method to identify septal scars in CRT candidates.

Disclosures

OAS is co-inventor of the "Method for myocardial segment work analysis", which was used to calculate myocardial work. The other authors have no disclosures.

CRediT authorship contribution statement

Camilla Kjellstad Larsen: Methodology, Formal analysis, Investigation, Writing – original draft, Visualization. **Elena Galli:** Formal analysis, Investigation, Writing – review & editing. **Jürgen Duchenne:** Formal analysis, Investigation, Writing – review & editing. **John M. Aalen:** Formal analysis, Investigation, Writing – review & editing. **Caroline Stokke:** Resources, Writing – review & editing, Visualization. **Jan Gunnar Fjeld:** Resources, Writing – review & editing, Visualization. **Ganna Degtiarova:** Formal analysis, Writing – review & editing. **Piet Claus:** Resources, Writing – review & editing. **Olivier Gheysens:** Resources, Writing – review & editing. **Jorg Saberniak:** Formal analysis, Writing – review & editing. **Per Anton Sirnes:** Formal analysis, Writing – review & editing. **Erik Lyseggen:** Resources, Writing – review & editing. **Jan Bogaert:** Resources, Writing – review & editing. **Erik Kongsgaard:** Resources, Writing – review & editing. **Martin Penicka:** Methodology, Resources, Writing – review & editing, Funding acquisition. **Jens-Uwe Voigt:** Methodology, Resources, Writing – review & editing, Funding acquisition. **Erwan Donal:** Methodology, Resources, Writing – review & editing, Funding acquisition. **Einar Hopp:** Methodology, Validation, Resources, Writing – review & editing, Visualization, Supervision, Funding acquisition. **Otto A. Smiseth:** Conceptualization, Methodology, Validation, Resources, Writing – review & editing, Visualization, Supervision, Project administration, Funding acquisition.

References

[1] M. Glikson, J.C. Nielsen, M.B. Kronborg, Y. Michowitz, A. Auricchio, I.M. Barbash, et al., 2021 ESC guidelines on cardiac pacing and cardiac resynchronization therapy: developed by the task force on cardiac pacing and cardiac resynchronization therapy of the European Society of Cardiology (ESC) with the special contribution of the European Heart Rhythm Association (EHRA), Eur. Heart J. 42 (35) (2021) 3427–3520.

[2] J.G. Cleland, J.C. Daubert, E. Erdmann, N. Freemantle, D. Gras, L. Kappenberger, et al., The effect of cardiac resynchronization on morbidity and mortality in heart failure, N. Engl. J. Med. 352 (15) (2005) 1539–1549.

[3] G.B. Bleeker, T.A. Kaandorp, H.J. Lamb, E. Boersma, P. Steendijk, A. de Roos, et al., Effect of posterolateral scar tissue on clinical and echocardiographic improvement after cardiac resynchronization therapy, Circulation. 113 (7) (2006) 969–976.

[4] J.M. Aalen, E. Donal, C.K. Larsen, J. Duchenne, M. Lederlin, M. Cvijic, et al., Imaging predictors of response to cardiac resynchronization therapy: left ventricular work asymmetry by echocardiography and septal viability by cardiac magnetic resonance, Eur. Heart J. 41 (39) (2020) 3813–3823.

[5] R.J. Kim, D.S. Fieno, T.B. Parrish, K. Harris, E.L. Chen, O. Simonetti, et al., Relationship of MRI delayed contrast enhancement to irreversible injury, infarct age, and contractile function, Circulation. 100 (19) (1999) 1992–2002.

[6] F.W. Prinzen, W.C. Hunter, B.T. Wyman, E.R. McVeigh, Mapping of regional myocardial strain and work during ventricular pacing: experimental study using magnetic resonance imaging tagging, J. Am. Coll. Cardiol. 33 (6) (1999) 1735–1742.

[7] S. Ono, R. Nohara, H. Kambara, K. Okuda, C. Kawai, Regional myocardial perfusion and glucose metabolism in experimental left bundle branch block, Circulation. 85 (3) (1992) 1125–1131.

[8] J. Duchenne, A. Turco, S. Ünlü, E.D. Pagourelias, K. Vunckx, G. Degtiarova, et al., Left ventricular remodeling results in homogenization of myocardial work distribution, Circ. Arrhythm. Electrophysiol. 12 (5) (2019), e007224.

[9] A. D'Andrea, P. Caso, R. Scarafile, L. Riegler, G. Salerno, F. Castaldo, et al., Effects of global longitudinal strain and total scar burden on response to cardiac resynchronization therapy in patients with ischaemic dilated cardiomyopathy, Eur. J. Heart Fail. 11 (1) (2009) 58–67.

[10] V. Delgado, R.J. van Bommel, M. Bertini, C.J. Borleffs, N.A. Marsan, C.T. Arnold, et al., Relative merits of left ventricular dyssynchrony, left ventricular lead position, and myocardial scar to predict long-term survival of ischemic heart failure patients undergoing cardiac resynchronization therapy, Circulation. 123 (1) (2011) 70–78.

[11] A.C. Kydd, F. Khan, D. Gopalan, L. Ring, B.S. Rana, M.S. Virdee, et al., Utility of speckle tracking echocardiography to characterize dysfunctional myocardium in patients with ischemic cardiomyopathy referred for cardiac resynchronization therapy, Echocardiography. 31 (6) (2014) 736–743.

[12] H. Engblom, J. Tufvesson, R. Jablonowski, M. Carlsson, A.H. Aletras, P. Hoffmann, et al., A new automatic algorithm for quantification of myocardial infarction imaged by late gadolinium enhancement cardiovascular magnetic resonance: experimental validation and comparison to expert delineations in multi-center, multi-vendor patient data, J. Cardiovasc. Magn. Reson. 18 (1) (2016) 27.

[13] M.J. Knuuti, P. Nuutila, J. Ruotsalainen, M. Saraste, R. Harkonen, A. Ahonen, et al., Euglycemic hyperinsulinemic clamp and oral glucose load in stimulating myocardial glucose utilization during positron emission tomography, J. Nucl. Med. 33 (7) (1992) 1255–1262.

[14] K. Russell, M. Eriksen, L. Aaberge, N. Wilhelmsen, H. Skulstad, E.W. Remme, et al., A novel clinical method for quantification of regional left ventricular pressure-strain loop area: a non-invasive index of myocardial work, Eur. Heart J. 33 (6) (2012) 724–733.

[15] M.D. Cerqueira, N.J. Weissman, V. Dilsizian, A.K. Jacobs, S. Kaul, W.K. Laskey, et al., Standardized myocardial segmentation and nomenclature for tomographic imaging of the heart. A statement for healthcare professionals from the cardiac imaging Committee of the Council on clinical cardiology of the American Heart Association, Circulation. 105 (4) (2002) 539–542.

[16] M.J. Garcia, R.Y. Kwong, M. Scherrer-Crosbie, C.C. Taub, R. Blankstein, J. Lima, et al., State of the art: imaging for myocardial viability: a scientific statement from the American Heart Association, Circ Cardiovasc Imaging. 13 (7) (2020), e000053.

[17] G. Degtiarova, P. Claus, J. Duchenne, J. Bogaert, J. Nuyts, G. Vöros, et al., Left ventricular regional glucose metabolism in combination with septal scar extent identifies CRT responders, Eur. J. Nucl. Med. Mol. Imaging 48 (8) (2021) 2437–2446.

[18] L.E. Sade, S. Saba, J.J. Marek, T. Onishi, D. Schwartzman, E.C. Adelstein, et al., The association of left ventricular lead position related to regional scar by speckle-tracking echocardiography with clinical outcomes in patients receiving cardiac resynchronization therapy, J. Am. Soc. Echocardiogr. 27 (6) (2014) 648–656.

[19] H. Mahrholdt, A. Zhydkov, S. Hager, G. Meinhardt, H. Vogelsberg, A. Wagner, et al., Left ventricular wall motion abnormalities as well as reduced wall thickness can cause false positive results of routine SPECT perfusion imaging for detection of myocardial infarction, Eur. Heart J. 26 (20) (2005) 2127–2135.

[20] E.C. Adelstein, H. Tanaka, P. Soman, G. Miske, S.C. Haberman, S.F. Saba, et al., Impact of scar burden by single-photon emission computed tomography myocardial perfusion imaging on patient outcomes following cardiac resynchronization therapy, Eur. Heart J. 32 (1) (2011) 93–103.

[21] C. Ypenburg, M.J. Schalij, G.B. Bleeker, P. Steendijk, E. Boersma, P. Dibbets-Schneider, et al., Impact of viability and scar tissue on response to cardiac resynchronization therapy in ischaemic heart failure patients, Eur. Heart J. 28 (1) (2007) 33–41.

[22] I. Morishima, K. Okumura, H. Tsuboi, Y. Morita, K. Takagi, R. Yoshida, et al., Impact of basal inferolateral scar burden determined by automatic analysis of 99mTc-MIBI myocardial perfusion SPECT on the long-term prognosis of cardiac resynchronization therapy, Europace. 19 (4) (2017) 573–580.